Supporting Information

Reversible Oxygen Incorporation in Metastable Bixbyite V_2O_3 Nanocrystals

Contents:

Experimental Supporting Information

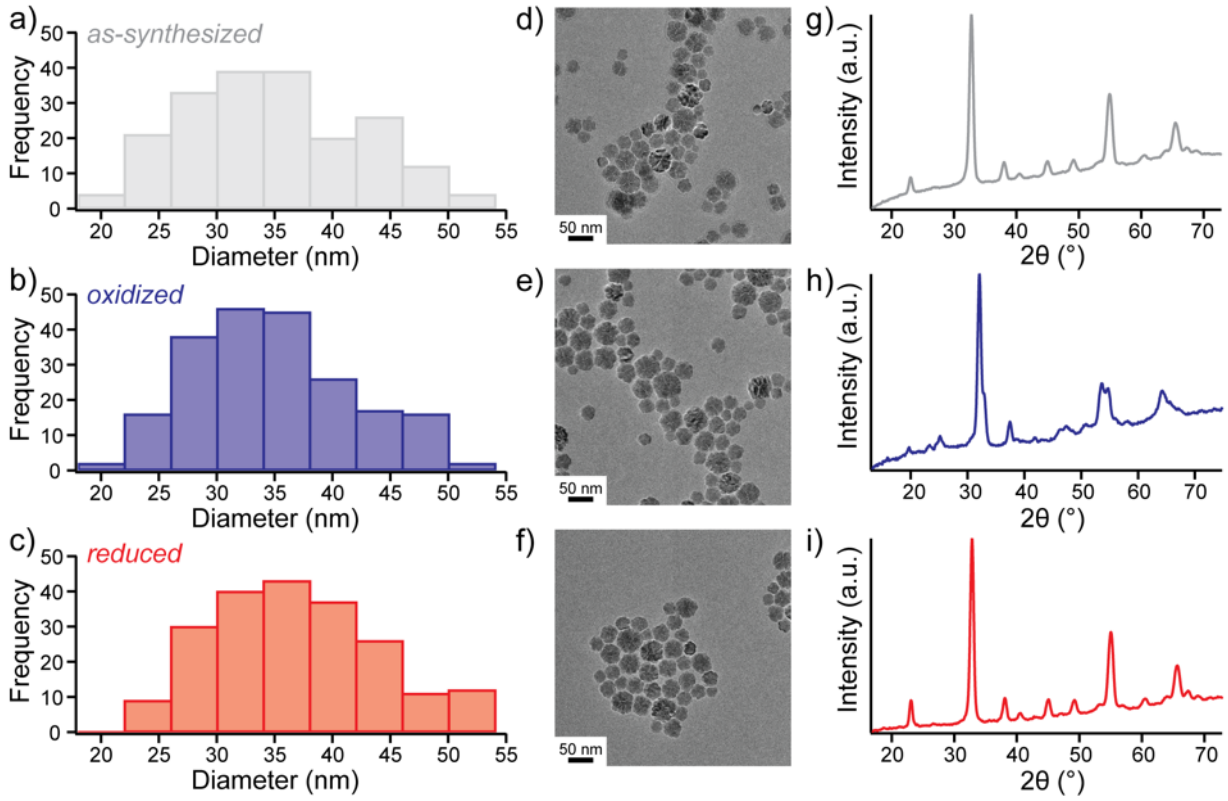

Figure S1. Size distribution histograms, representative TEM images, and XRD patterns of as-synthesized NCs (a,d,g), NCs oxidized in air at 125°C for 2 hours (b,e,h), and NCs reduced after oxidation by annealing in nitrogen at 325°C for 1 hour (c,f,i). The average NC diameter of each sample is 31.0 ± 6.9 nm, 31.0 ± 7.5 nm, and 33.1 ± 7.4 nm, respectively, with over 200 NCs measured by TEM for each.

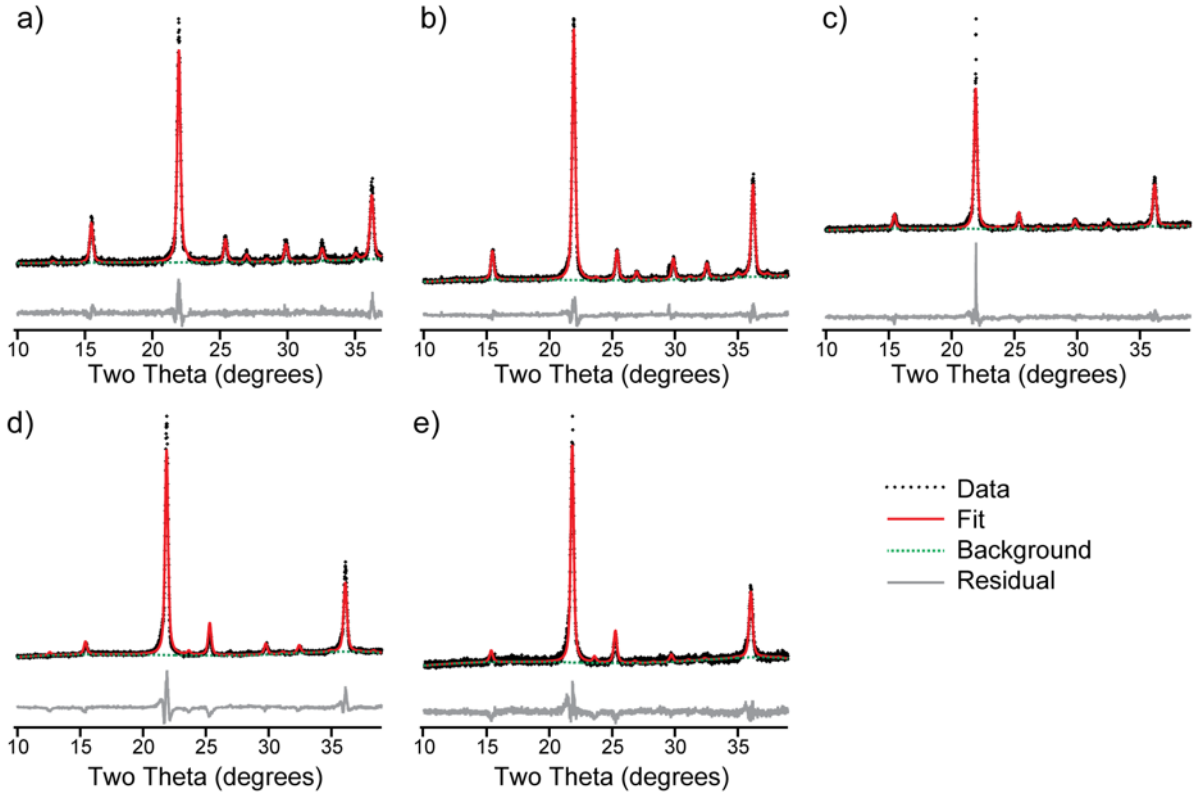

Figure S2. Rietveld refinement fits and residuals for samples annealed in air at 125°C for a) 0, b) 10, c) 20, d) 30, and e) 40 minutes.

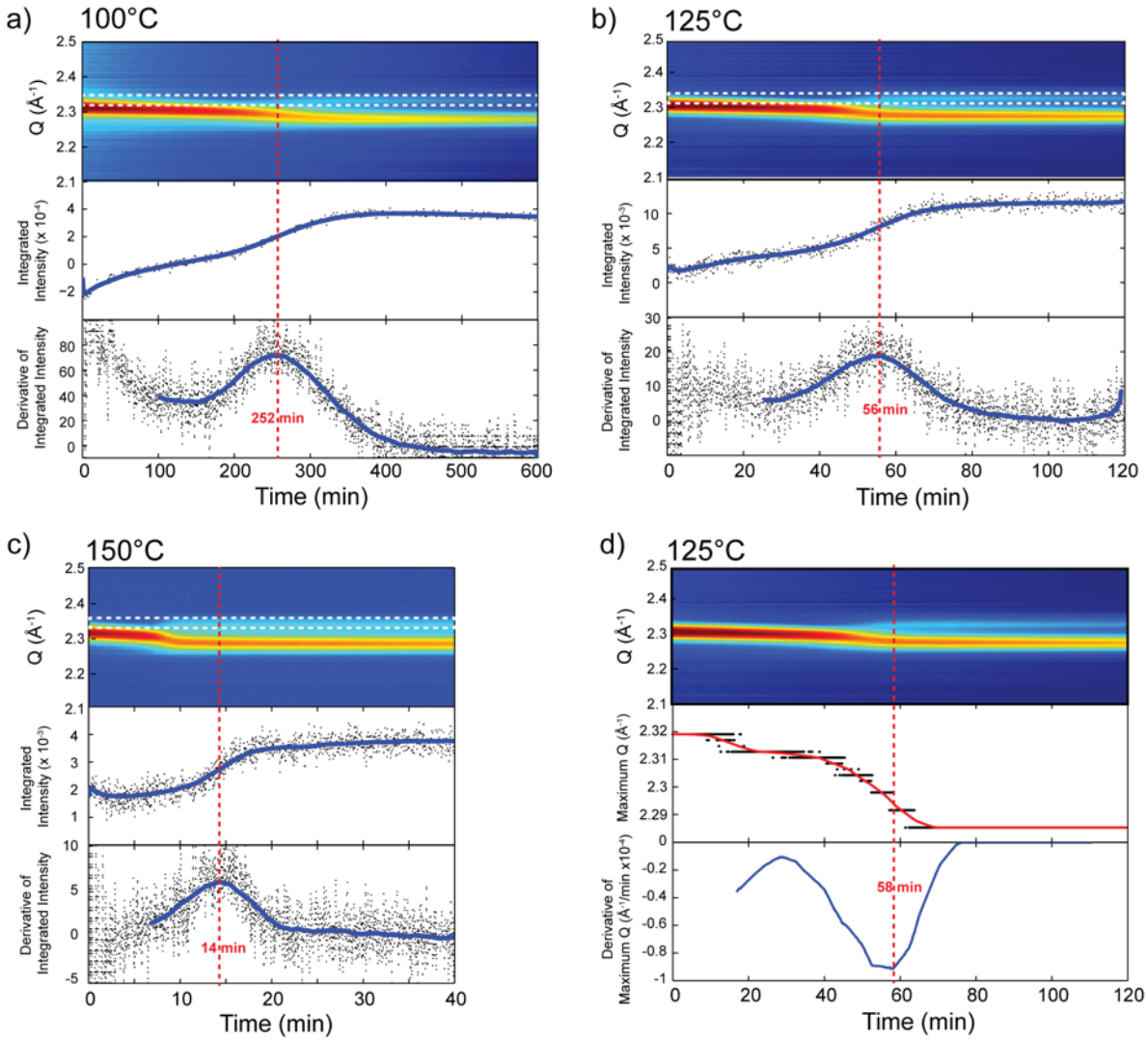

Figure S3. Determination of transformation time from maximum first derivative of shoulder peak intensity (area between white dotted lines) with respect to time for isotherms at a) 100°C, b) 125°C, and c) 150°C. d) Transformation time could also be determined from the minimum first derivative of peak position with respect to time as shown for the isotherm at 125°C. Both methods yield similar results.

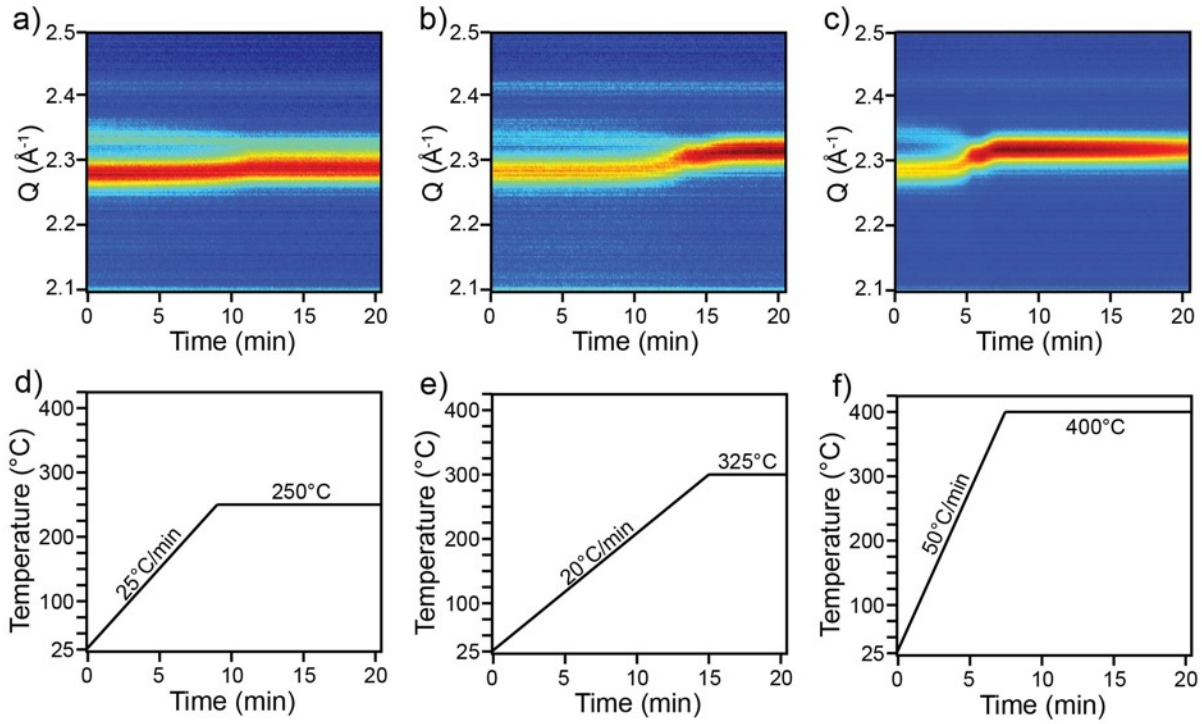

Figure S4. Reduction of oxidized bixbyite as observed by *in situ* XRD under helium flow (a, b, and c) and corresponding temperature profiles (d, e, and f). The peak present at ~2.1 and 2.42 in all samples is from the beryllium dome.

The figure above shows *in situ* XRD scans from an already oxidized and transformed sample heated under helium flow at 250, 325, and 400°C. The characteristic peak and shoulder of the unknown phase merge into one peak, characteristic of the bixbyite phase. The position of the peak after reduction is dependent on temperature, with higher temperatures resulting in peak positions closer to that of stoichiometric bixbyite and faster reduction kinetics.

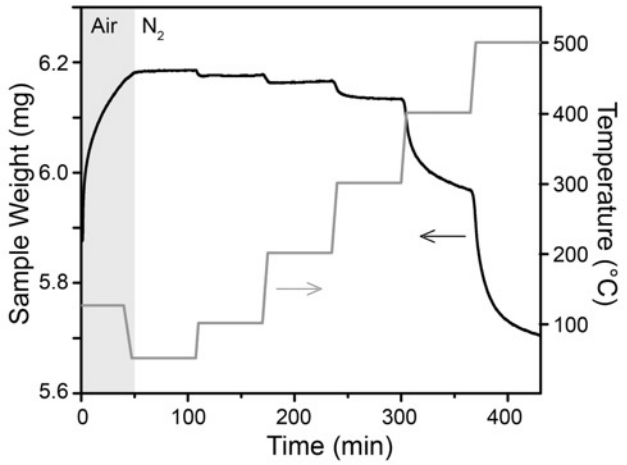

Figure S5. TGA scan showing initial oxidation (125°C for 50 min) followed by reduction of bixbyite NCs. Weight loss was measured (left axis) as temperature was increased by intervals of 100°C up to 500°C, with the temperature shown on right axis. Ligands were decomposed prior to TGA scan, by annealing in a tube furnace at 400°C for 2 hours in nitrogen.

Under nitrogen flow, weight loss was measured as temperature was increased by steps of 100°C. Initial weight loss at 100 and 200°C is minimal, but increases with temperature such that the largest decrease in weight occurs at 500°C. The equilibrium concentration of oxygen interstitials is clearly dependent on both atmosphere and temperature, with higher temperatures resulting in lower excess oxygen, δ, during the reduction process in inert gas.

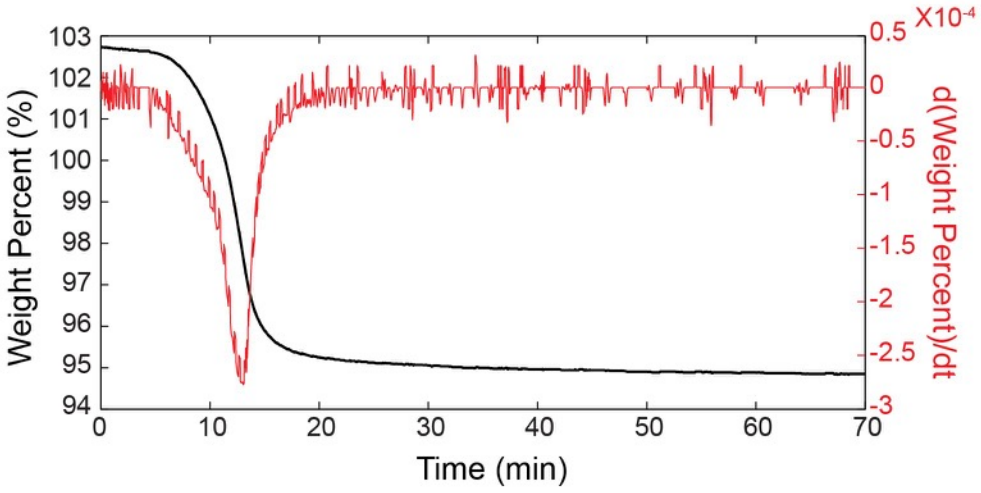

Figure S6. Weight percentage (black/left) and derivative of weight percentage with respect to time (red/right) as a function of time while heating in nitrogen to 325°C. The maximum change in weight occurs at approximately 13 minutes, at which point the temperature is still ramping and is equal to 310°C. This is the same time at which a rapid change in lattice parameter is observed by in situ XRD, and thus, likely corresponds to a point at which a large amount of oxygen exits the lattice.

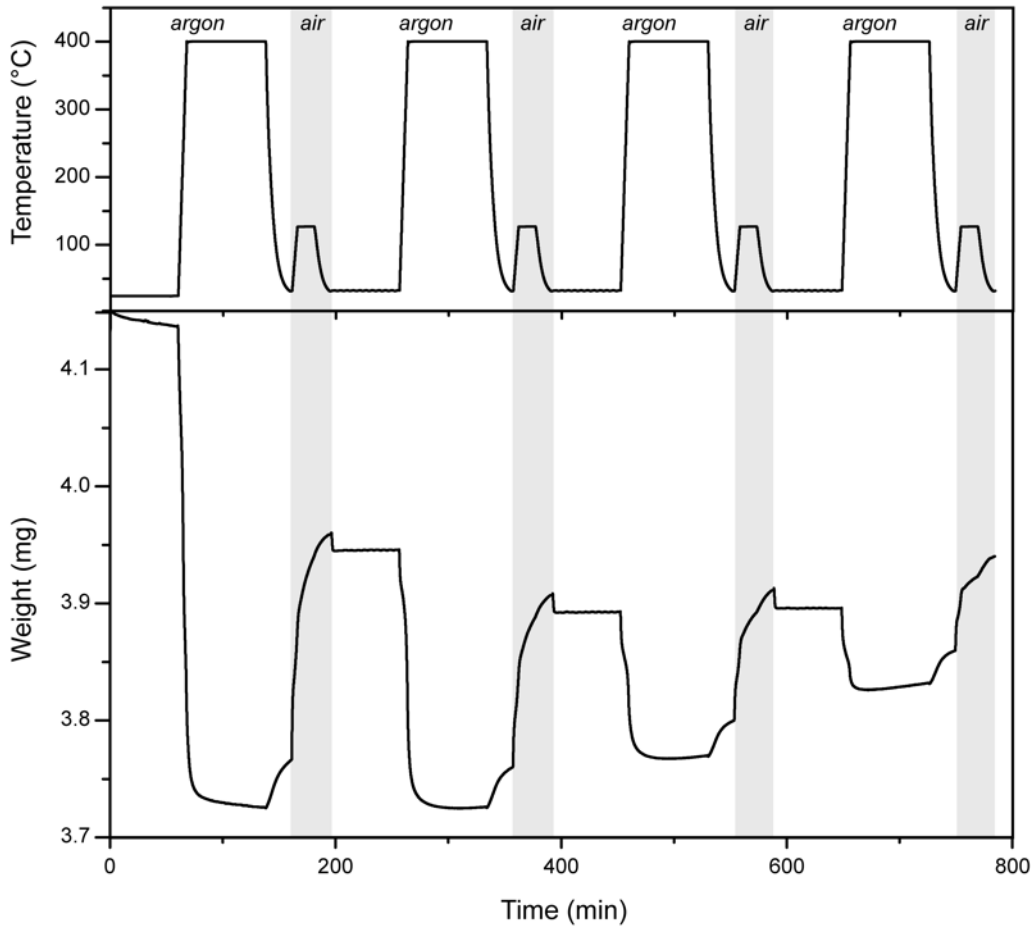

Figure S7. TGA scan while cycling between argon flow at 400°C and air flow at 125°C with large initial weight loss due to ligand decomposition.

Density Functional Theory

Table S1. Exchange Correlation Functional Testing

	Volume (Å^3)			**Band Gap (eV)**			**ΔE0/f.u. vs. monoclinic (eV)**		
Functional	Mon.	Cor.	Bix.	Mon.	Cor.	Bix.	Mon.	Cor.	Bix.
PBEsol (V_pv)	*202.75*	*306.01*	*841.13*	*0.285*	0.032	*0.155*	*0*	*0.067*	*0.071*
PBEsol (V_sv)	*202.32*	*305.29*	*839.37*	*0.293*	0.035	*0.155*	*0*	*0.069*	*0.079*
PBE	210.91	318.18	871.70	*0.666*	0.086	*0.532*	0	0.057	-0.003
PW	210.04	316.79	*868.96*	*0.562*	*0.007*	*0.432*	0	0.056	0.004
LDA	*194.37*	*294.51*	*803.16*	0.029	0.026	0.003	*0*	*0.100*	*0.184*
experiment	199.94	296.94	829.68	0.6	0	>0	0	>0	>cor.

A variety of exchange correlation functionals and pseudopotentials were tested to determine the one that most closely matched experimental values. The PBEsol and LDA functionals were found to perform the best with respect to unit cell volumes, with the results within ±5% of experiment italicized. These two functionals also described the energetics correctly, with monoclinic phase having the lowest energy per formula unit, followed by corundum phase, then finally bixbyite. However, the functionals which performed well with respect to volume and energy failed to describe the electronic properties of the materials correctly. At the very least, the semiconducting monoclinic and bixbyite phases should have a band gap greater than zero, and the metallic corundum phase should have a band gap of zero. The functionals satisfying these conditions are italicized, with the PW functional performing best. The PBEsol functional with V_sv pseudopotential was chosen for the remainder of the calculations, as structure and energetics are most important for this study. This testing was done with spin polarization for all phases and an antiferromagnetic moment set for the monoclinic phase, but not yet for bixbyite.[1] The U and J values used here were U=2.8 and J=0.93, values which have been used in previously in the literature.[2]

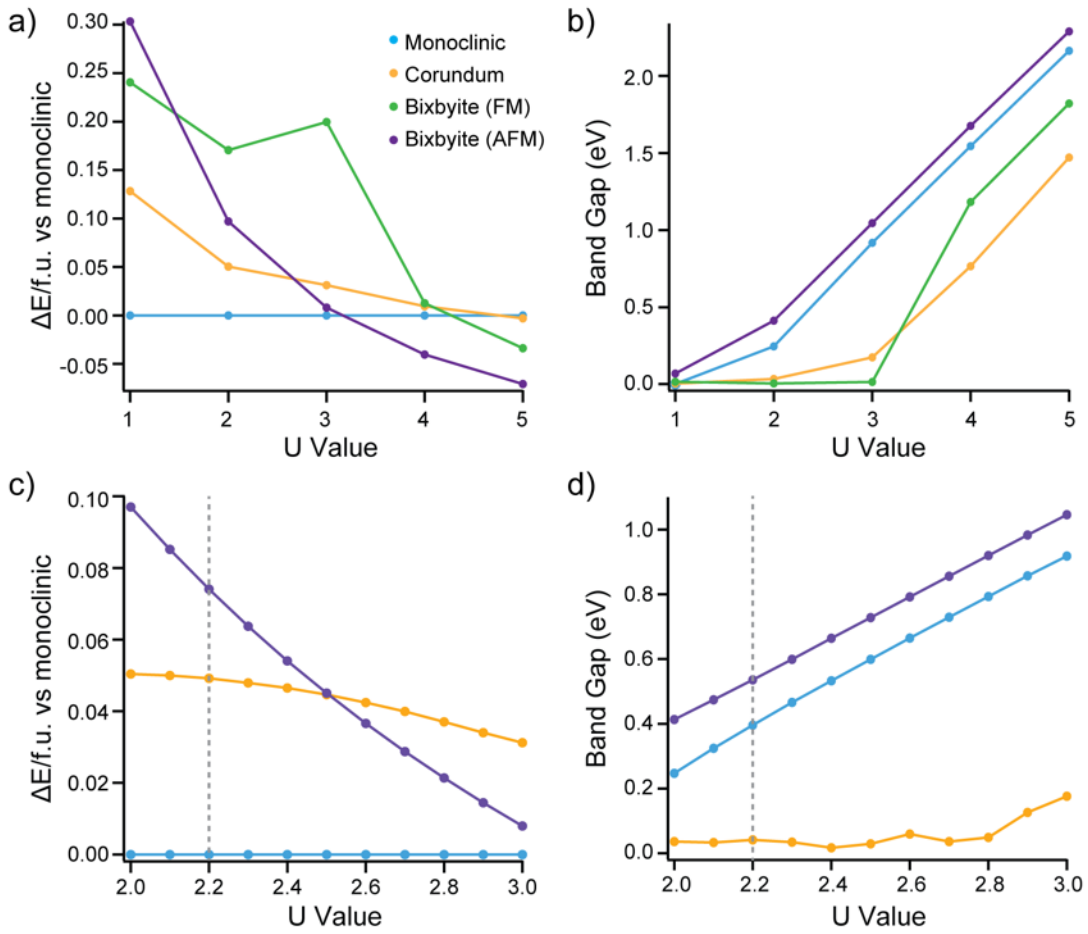

Figure S8. a) The change in energy per formula unit versus the monoclinic phase and b) band gap plotted as a function of U value, finer detail in c) and d)

Polymorph stability (a) and bandgap (b) were first determined over a coarse range of Dudarev-type U values between 1 and 5. In terms of polymorph stability, monoclinic phase should have the lowest energy, followed by corundum phase then bixbyite. This is true for values below 4 in the case of bixbyite without antiferromagnetic (AFM) ordering and below 3 for bixbyite with AFM ordering. U must be kept below 3 to accurately describe the metallic nature of corundum phase, however this also results in a band gap of zero for bixbyite without AFM ordering. Therefore, AFM ordering in bixbyite is necessary to concurrently describe the electronic structure of corundum and bixbyite.

The analysis was repeated for U values between 2 and 3. U values of 2.5 and greater are ruled out because bixbyite becomes more stable than corundum at these values. Corundum should have a band gap of zero, ruling out U values above 2.8. The monoclinic phase's band gap of 0.6 eV is matched at U=2.5, but this does not describe the energetics well. In order to best describe both energetics and band gap, the value of U=2.2 was chosen.

Table S2. Magnetic Ordering in Bixbyite

Ordering		**Volume (Å^3)**	**Band Gap (eV)**	**ΔE0 (eV)**
No spin polarization		772.25	0.000	-668.25
Ferromagnetic		839.37	0.155	-702.91
Antiferromagnetic	a	832.99	0.661	-704.14
	b	833.11	0.653	*-704.19*
	c	833.65	0.166	-703.35
	d	833.94	0.608	-704.00
Experiment		829.68	>0	

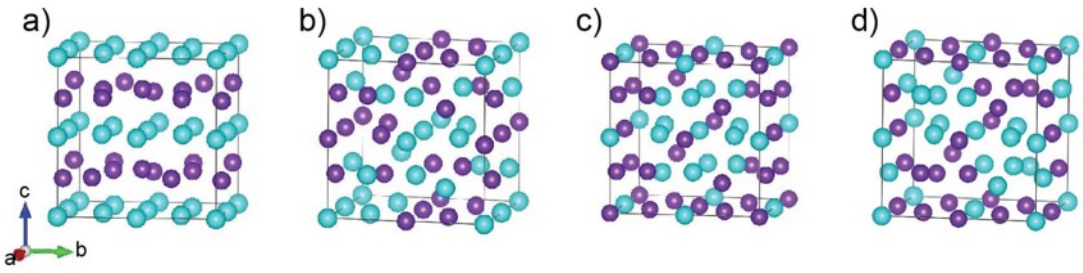

Antiferromagnetic ordering yields the highest band gaps and lowest energies. Several collinear orderings were tested, the ones which converged are listed in the table and shown in the figure above, with blue atoms representing spin up and purple is spin down. The ordering with the lowest overall energy, labeled b, was chosen. These tests were done with U and J values of 2.8 and 0.93, respectively. The chosen ordering is such that all nearest neighbor vanadium atoms in d-sites have opposing spins.

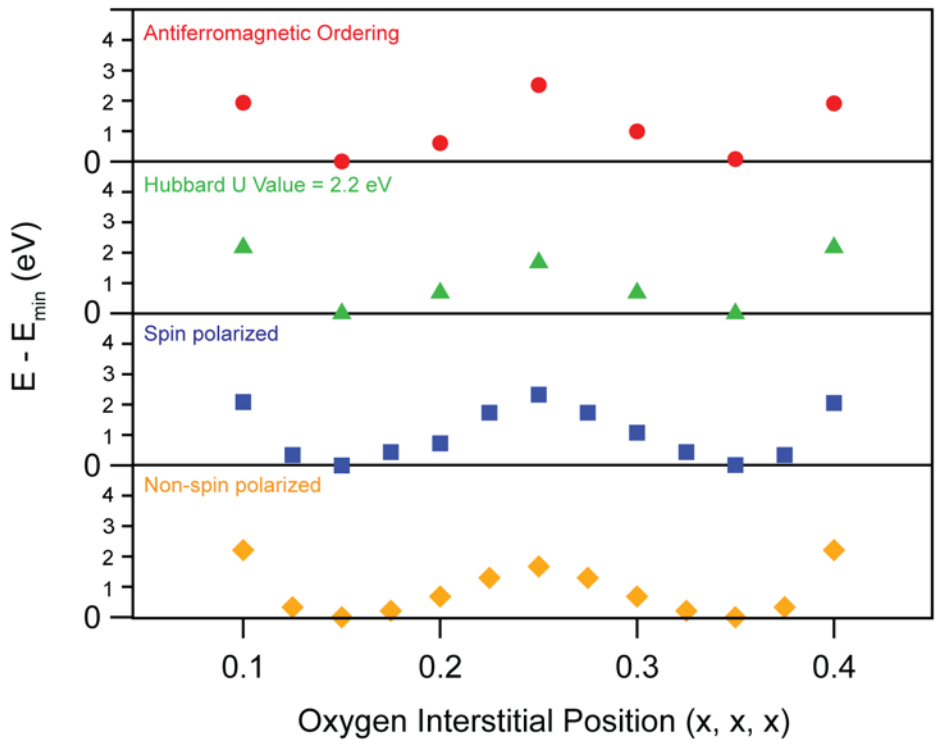

Figure S9. Oxygen interstitial mapping along the body diagonal of the bixbyite lattice

This analysis was done in **Figure 3** of the main text without spin polarization and with a different U and J value than was used for the rest of the analysis (U=2.8 and J=0.93). Therefore, this analysis was repeated with spin polarization, antiferromagnetic ordering, and the U value of 2.2 for the case of interstitials placed along the body diagonal. The resulting energies (relative to minimum) are quite similar, with minima occurring at (0.15, 0.15, 0.15) and (0.35, 0.35, 0.35) in all cases.

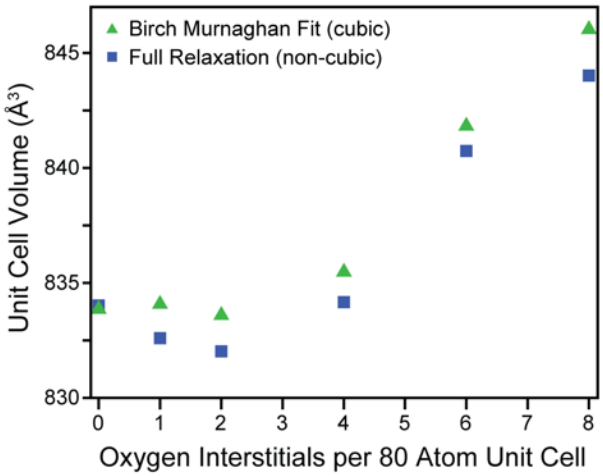

Figure S10. Volume expansion as a function of oxygen interstitial concentration as calculated by DFT

The equilibrium unit cell volume of bixbyite with differing amounts of oxygen interstitials was obtained by full relaxation (leading to a subtle trigonal distortion) and by using a Birch Murnaghan fit to fix cubic shape (**Figure S11**). At lower levels of oxygen interstitials, cell volume remains largely unchanged, while at higher levels, the volume rapidly increases. This non-linear trend agrees with experiment; however a larger number of oxygen interstitials is required before expansion occurs.

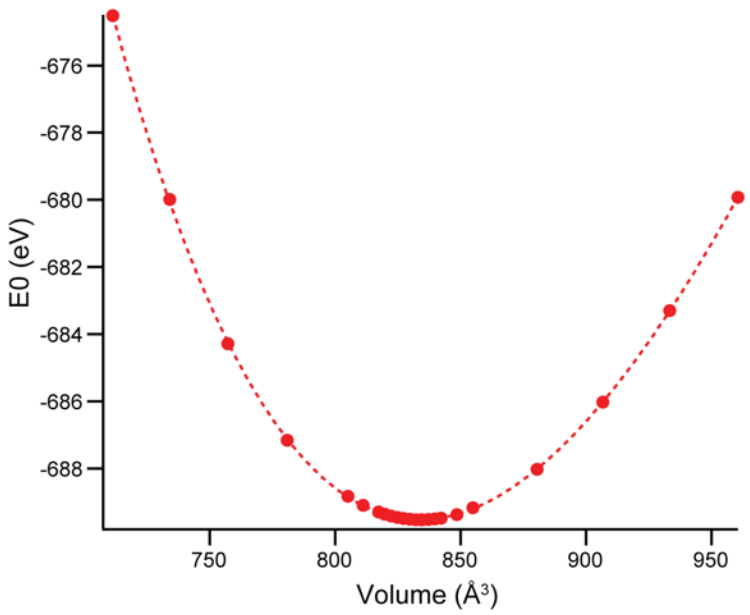

Figure S11. Bixbyite unit cell energy as a function of volume. The data was fit to the Birch Murnaghan equation (dashed line) using the parameters below.

Table S3. Birch Murnaghan Fitting Parameters

Parameter	Value
E0 (eV)	-689.52
V0 (Å^3)	834.19 ± 0.0307
B0 (eV/ Å^3)	1.29
B0' (dB/dP)	4.78

To determine the equilibrium lattice parameter of the cubic bixbyite unit cell, the Birch Murnaghan equation was employed[3]:

$$E(V) = E_0 + \frac{9V_0B_0}{16}\left\{\left[\left(\frac{V_0}{V}\right)^{\frac{2}{3}} - 1\right]^3 B'_0 + \left[\left(\frac{V_0}{V}\right)^{\frac{2}{3}} - 1\right]^2 \left[6 - 4\left(\frac{V_0}{V}\right)^{\frac{2}{3}}\right]\right\}$$

Where E_0 is the equilibrium energy of the cell, V_0 is the equilibrium volume, B_0 is the elastic modulus, and B_0' is the derivative of elastic modulus with respect to volume. Cell volume, V, was fixed and ion positions were relaxed, yielding cell energy, E. This was repeated for a range of volumes, and the resulting energy vs. volume curve was fit to the Birch Murnaghan equation to determine equilibrium volume and energy.

References

(1) Ezhov, S. Y.; Anisimov, V. I.; Khomskii, D. I.; Sawatzky, G. A. Orbital Occupation, Local Spin, and Exchange Interactions in V_2O_3. *Phys. Rev. Lett.* **1999**, *83* (20), 4136–4139.
(2) Solovyev, I.; Hamada, N.; Terakura, K. t_{2g} versus All 3*d* Localization in La*M*O_3 Perovskites (*M*=Ti-Cu): First-Principles Study. *Phys. Rev. B* **1996**, *53* (11), 7158–7170.
(3) Birch, F. Finite Elastic Strain of Cubic Crystals. *Phys. Rev.* **1947**, *71* (11), 809–824.